remote sensing

Article

Determination of Crop Water Stress Index by Infrared Thermometry in Grapefruit Trees Irrigated with Saline Reclaimed Water Combined with Deficit Irrigation

Cristina Romero-Trigueros [1,*], José María Bayona Gambín [2], Pedro Antonio Nortes Tortosa [2], Juan José Alarcón Cabañero [2] and Emilio Nicolás Nicolás [2]

[1] Department of Agricultural and Environmental Science, University of Bari "Aldo Moro", Campus, Via Amendola 165/A, 70126 Bari, Italy

[2] Department of Irrigation, Centro de Edafología y Biología Aplicada del Segura, CSIC, P.O. Box 164, 30100 Espinardo, Murcia, Spain; jmbayona@cebas.csic.es (J.M.B.G.); panortes@cebas.csic.es (P.A.N.T.); jalarcon@cebas.csic.es (J.J.A.C.); emilio@cebas.csic.es (E.N.N.)

* Correspondence: cromero@cebas.csic.es

Received: 22 February 2019; Accepted: 25 March 2019; Published: 28 March 2019

Abstract: Water is not always accessible for agriculture due to its scarcity. In order to successfully develop irrigation strategies that optimize water productivity characterization of the plant, the water status is necessary. We assessed the suitability of thermal indicators by infrared thermometry (IRT) to determine the water status of grapefruit in a commercial orchard with long term irrigation using saline reclaimed water (RW) and regulated deficit irrigation (RDI) in Southeastern Spain. The results showed that Tc-Ta differences were positive in a wide range of vapor pressure deficits (VPD), and the major Tc-Ta were found at 10.00 GMT, before and after the highest daily values of VPD and solar radiation, respectively, were reached. In addition, we evaluated the relationships between Tc-Ta and VPD to establish the Non-Water Stressed Baselines (NWSBs), which are necessary to accurately calculate the crop water stress index (CWSI). Two important findings were found, which include i) the best significant correlations ($p < 0.005$) found at 10.00 GMT and their slopes were positive, and ii) NWSBs showed a marked hourly and seasonal variation. The hourly shift was mainly explained by the variation in solar radiation since both the NWSB-slope and the NWSB-intercept were significantly correlated with a zenith solar angle (θZ) ($p < 0.005$). The intercept was greater when θZ was close to 0 (at midday) and the slope displayed a marked hysteresis throughout the day, increasing in the morning and decreasing in the afternoon. The NWSBs determination, according to the season improved most of their correlation coefficients. In addition, the relationship significance of Tc-Ta versus VPD was higher in the period where the intercept and Tc-Ta were low. CWSI was the thermal indicator that showed the highest level of agreement with the stem water potential of the different treatments even though Tc and Tc-Ta were also significantly correlated. We highlight the suitability of thermal indicators measured by IRT to determine the water status of grapefruits under saline (RW) and water stress (RDI) conditions.

Keywords: canopy temperature; IRT sensor; saline stress; stem water potential

1. Introduction

Citrus is one of the most important commercial fruit crops in the world, including Southeastern Spain, where the climate is semi-arid Mediterranean and water is not always accessible due to its scarcity. It is well known that water availability is becoming the most limiting factor for crop production in most countries of the world [1] while the demand for food will increase as a result of increasing population and dietary changes [2]. Hence, in the near future, the need to manage irrigation efficiently gains special importance. New tools and strategies that enable the optimization of water productivity will be highly sought after and will need to be developed [3].

In order to overcome this problematic scarcity of water resources for agriculture, the use of non-conventional water sources such as reclaimed water (RW) could become an alternative for farmers [4] since these waters are beneficial to crops when used as fertilizers due to their high macronutrient concentration [5] even though an excess of them could promote their loss through leaching [6]. The worldwide use of RW is being developed very rapidly, mainly in arid and semi-arid agroecosystems. Currently, approximately 4% of all RW is reused in the world and it is foreseen that, by 2030, RW will represent 1.66% (26 billion m^3 per year) of the total water use [7]. More specifically, in Murcia, which is a semi-arid region located in Southern Spain, there are 93 operational wastewater treatment plants (WWTP) that deliver almost 109 hm^3 per year [8]. Thus, RW can be considered as a continuous and cheap source of water for agriculture in the region. Conversely, RW may create risks for agriculture since it often has a high concentration of different salts. An unbalanced supply of micro-nutrients from RW may cause nutritional excess of any of them, including Mn, Zn, Cu, B, Na, and Cl^- [9]. Therefore, an inappropriate management of irrigation with RW can exacerbate the negative impacts on plant physiology and growth [10]. More specifically, the negative effects of salinity and water stress on leaf gas exchange and chlorophyll content have been reported in citrus [11].

Another useful technique for optimizing water productivity currently in use is the regulated deficit irrigation (RDI) strategy, where water deficits are imposed during phenological periods when the plant is the least sensitive to water stress, with little or no impact on fruit yield or quality. When RDI is applied, the irrigation regime must be monitored in order to optimize water productivity while maintaining good yield and positive economic returns to growers [3].

In order to successfully mitigate the scarcity of water for irrigation, both RW and RDI strategies need the reliable characterization of the plant water status.

The traditional water stress indicators used for trees such as water potential (Ψ) or stomatal conductance (g_s) are time consuming, must be performed manually, and provide point measurements including a single location of soil, a leaf, branch, or tree. They are incapable of truly representing the water status of an entire orchard without being financially impractical due to the number of monitoring sites required. In addition, the reliability of the information provided by Ψ decreases in species with isohydric behavior such as in citrus, since they have an efficient stomatal regulation that avoids marked decreases in water potential under conditions of low soil water or high evaporative demand [12].

Alternative methods that utilize remote sensing techniques and less laborious and amenable for automation are being sought for use in commercial orchards [13]. Remote sensing takes on a special significance within this context since it enables a better monitoring of large cultivated areas that make it easier to assess the precise management of the plant´s water stress. This has been extensively pointed out in the literature as a key factor for ensuring the success of water-saving irrigation strategies based on irrigation of plants below their full water requirements [14].

In this sense, measurements of the canopy temperature (Tc) by infrared thermometry (IRT) as an indicator of water stress are being increasingly used. The infrared remote temperature sensors (IRTs) provide a non-contact means of measuring the surface temperature of plants. This method allows the measurements of large areas to detect plant leaf temperatures continuously. It can be manually handled [15] or remotely used and mounted on a mast or a crane [16,17] over an aerial platform [18] or on a satellite [19]. At present, these are relatively fast and cheap, easily automated, and can be installed permanently in fields. Furthermore, IRTs can be positioned in a way that they see only tree foliage [3,16].

Canopy temperature obtained by IRTs and its related thermal indicators such as Crop Water Stress Index (CWSI) and Stomatal Conductance Index (I_g) have been known to be a simple, cost-effective proxy for monitoring crop water status for many years [15,20].

CWSI is based on the relationship between actual Tc and the theoretical values of Tc under two boundary conditions, which are dependent on the vapor pressure deficit (VPD) including a lower limit when plant transpires at its maximum rate (fully irrigated trees with stomata fully opened) and an upper limit under no transpiration (tree under maximum water stress conditions and stomata completely closed). The lower limit is described by a linear regression between Tc-Ta and VPD, which is known as the Non Water Stress Baseline (NWSB). The method widely used to define the upper limit is proposed by Reference [21], which use a horizontal line departing at the intercept of NWSB corrected for air temperature. This empirical baseline used to calculate the index, especially the NWSB, are stable under the environmental conditions expected during the irrigation season. If instability is found, the variation in the baseline should be predictable. Therefore, the errors in CWSI can be minimized. In addition, dry, stable weather conditions are desirable for avoiding important errors in defining the CWSI. For this reason, one of the limitations of the CWSI is that its precision is climate-dependent.

In citrus, it has been shown that canopy temperature can be used to detect plant water stress [22–25]. Nevertheless, it is known that citrus trees are sensitive to the air vapor pressure, which reduces transpiration in conditions of high VPD [10] and makes the use of this method in such conditions more difficult [13].

The CWSI concept has been applied in many studies to detect water stress, mostly in annual crops and most recently in woody crops [3,26–28]. However, few studies have used CWSI to assess saline stress [29]. In citrus crops, based on our knowledge, there are only two published reports on the use of CWSI under water stress such as in sweet lime [30] and in oranges and mandarins [26]. Another study in orange trees was unable to characterize the CWSI under contrasting water regimes using thermography [23]. However, nothing has been published about grapefruit trees. Thus, it would be necessary to continue research in this field, given the potential usefulness of the CWSI for remote sensing applications. We hypothesized that the use of Tc measured by IRT and its derived CWSI can be useful for evaluating both water and the saline stress of grapefruit trees irrigated with RW and RDI. In order to verify this hypothesis and improve the lack of knowledge on the use of NWSB to calculate the CWSI in citrus, more specifically grapefruit, this work intends to (i) assess the diurnal course patterns of Tc and Tc-Ta oscillations measured by thermometry in trees under long term water and saline stress, (ii) establish the non-water stressed baseline (NWSB) as well as its diurnal and seasonal time courses, and (iii) evaluate the suitability of the derived CWSI and define the most advisable thermal indicator (Tc, Tc-Ta, CWSI) correlated with plant water status by considering their irrigation treatment.

2. Materials and Methods

2.1. Experimental Area

The experiment was conducted at a commercial citrus orchard, located to the Northeast of the Murcia region in Campotéjar, 7 km north of Molina de Segura (38°07′18′′N, 1°13′15′′W) 132 m above sea level) with a BSkclimate by Köppen-Geiger classification [31] during the studied season (2017). The experimental plot of 0.5 ha was cultivated with 13-year-old 'Star Ruby' grapefruit trees (Citrus paradisi Macf) grafted onto Macrophylla rootstock (Citrus macrophylla) planted at 6 × 4 m. The irrigation was scheduled on the basis of daily evapotranspiration of the crop (ET_c) accumulated during the previous week. ET_c values were estimated by multiplying reference evapotranspiration (ET_0), (Figure 1), calculated with the Penman-Monteith methodology, via a monthly local crop coefficient, according to Reference [32]. The correction coefficient for ground cover was one, according to Reference [33]. All trees received the same amount of fertilizers, which were applied through the drip irrigation system of 215 kg N, 110 kg P_2O_5 and 150 kg K_2O $ha^{-1} \cdot year^{-1}$. Weeds were eradicated in the orchard by applying the farmers' commonly used pest control methods.

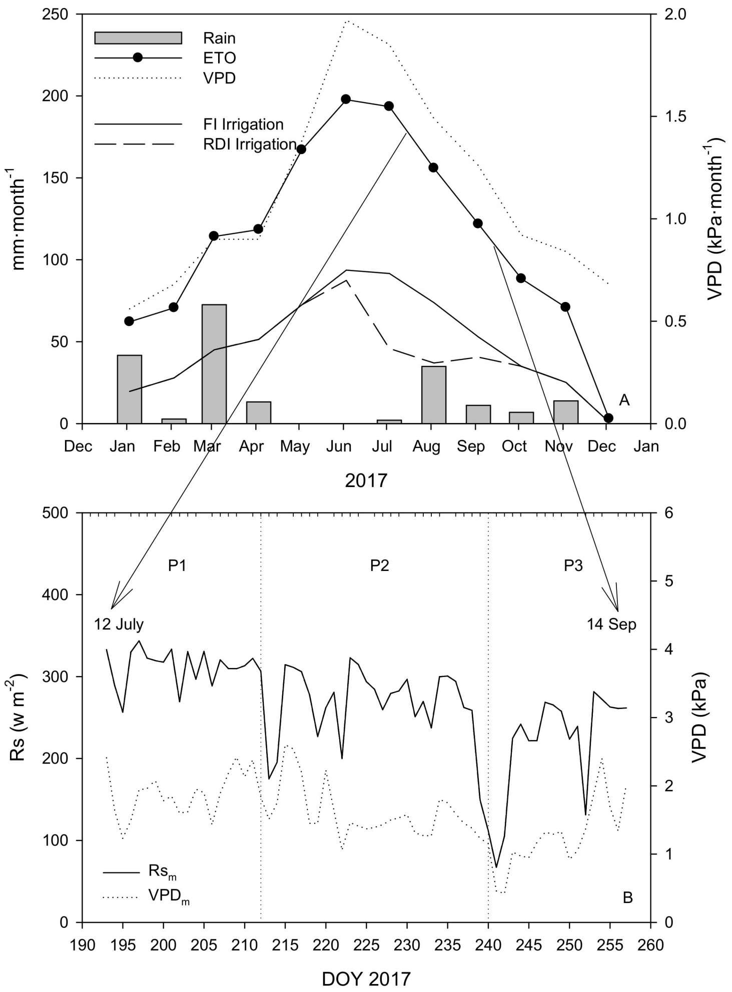

Figure 1. (**A**) Seasonal evolution of rainfall (mm·month^{-1}), full and regulated deficit irrigation (mm · month^{-1}), reference evapotranspiration (ET_0, mm · month^{-1}), and vapor pressure deficit (VPD, kPa · month^{-1}) during 2017. (**B**) Daily mean of VPD and solar radiation (Rs_m, w·m^{-2}) during the experimental period (from DOY 193 to 257 of year 2017). The discontinuous vertical lines divide the experimental period into three periods with a different water stress level: Period 1 (P1, DOY 193-212), Period 2 (P2, DOY 213-239), and Period 3 (P3, DOY 240-257).

2.2. Irrigation Treatments

The experimental plot was irrigated with two different water sources since 2007. In one case, water was pumped from the Tajo-Segura canal (transfer water, TW) and, in the other case, water was pumped from the North of "Molina de Segura" tertiary WWTP (reclaimed water, RW). The latter had high salt and nutrient levels (Table 1) with a high electrical conductivity (EC) close to 4 dS·m^{-1}, while, for the transfer irrigation water, the EC values were close to 1 dS·m^{-1}. Saline water was automatically mixed with water from TW at the irrigation control-head to lower its EC to ≈3 dS·m^{-1} in order to establish a constant EC during the experiment. This high level of salinity observed in the RW was mainly due to the high concentration of Cl^- and Na (Table 1). The boron concentration in RW was considerably higher than that in TW. Moreover, higher concentrations of N, P, and K were observed in RW than in TW. The pH was more basic in TW than RW (Table 1) and no differences in the concentration of heavy metals were found between two irrigation water sources (data not shown).

Table 1. Physical and chemical properties for Tajo-Segura transfer water and reclaimed water in 2017.

Property	Units	TW	RW
EC	**dS m^{-1}**	1.32 ± 0.38	3.97 ± 1.07
pH		8.33 ± 0.16	7.90 ± 0.18
Ca	**meq·L^{-1}**	4.49 ± 1.15	7.84 ± 2.52
Mg	**meq·L^{-1}**	4.69 ± 1.65	10.53 ± 4.21
K	**mg·L^{-1}**	0.16 ± 0.07	0.99 ± 0.20
Na	**meq·L^{-1}**	4.95 ± 2.78	21.00 ± 6.75
B	**mg·L^{-1}**	0.13 ± 0.09	0.79 ± 0.34
Cl^-	**meq· L^{-1}**	3.75 ± 2.04	18.98 ± 5.83
$NO_3{}^-$	**mg·L^{-1}**	3.88 ± 1.91	9.54 ± 6.51
$PO_4{}^-$	**mg·L^{-1}**	1.00 ± 0.00	1.37 ± 0.69
$SO_4{}^-$	**meq·L^{-1}**	5.44 ± 2.52	15.55 ± 6.99

Values are averages ± SD of 12 individual samples taken throughout the crop cycle. EC: electrical conductivity (dS·m^{-1}), RW: reclaimed water, TW: transfer water.

Two irrigation treatments were established for each water source. The first treatment was a full irrigation control (FI) irrigated throughout the growing season to fully satisfy crop water requirements (100% ET_c). The second one was a regulated deficit irrigation (RDI) treatment with an irrigation regime similar to FI, except during the second stage of fruit development when it received half the water, as applied to the FI (50% ET_c). The amount of water applied in 2017 was 4751.3 and 3738.1 m^3·ha^{-1} for FI and RDI treatments, respectively. Therefore, the RDI treatment saved about 21% of irrigation water. The RDI period began on DOY 185 (4 July, 2017) and ended on DOY 260 (17 September, 2017).

Our period of experimentation was included in the RDI period and ranged from DOY 212 to DOY 257. For a better understanding of the data that NWSBs are climate-dependent, the experimental period was divided into three sub-periods including Period 1 (P1, DOY 193-212), Period 2 (P2, 213-239), and Period 3 (P3, 240-257) based on changes in the solar radiation (Rs) and vapor pressure deficit (VPD) parameters, which are the most influential in NWSBs, which will be shown below. As depicted in Figure 1B, Rs and VPD values were quite similar within each subperiod. The average values were 312, 267, and 218 W·m^{-2} for Rs and 1.9, 1.6, and 1.3 kPa for VPD for each period, respectively. Both parameters decreased throughout the experiment.

2.3. Field Data Collection

Stem water potential (Ψ_s) were determined at midday every 15 days on eight fully-expanded leaves from the mid-shoot area per treatment (one leaf per tree and replicate), using a pressure chamber (model 3000, Soil Moisture Equipment Corp., California, USA), according to Reference [34], in leaves close to the trunk, which had been bagged within foil-covered aluminum envelopes at least 2 hours before the measurement [35].

Canopy temperatures were measured continually using thermometry. Infrared Remote Temperature Sensors (IRTs) (Apogee instruments, Utah, USA, model SIF-111) were mounted over one representative tree per replicate to capture the canopy temperature (Tc) continuously. The sensors had an angular field of view of 22° (half angle) and the accuracy over the calibrated range was ± 0.2 °C. A value of 0.96 was assumed for the emissivity to calculate Tc. Each sensor was mounted on aluminum masts with a horizontal mounting arm that ended up over the center of the canopy. To minimize solar radiative effects, sensors were protected by a PVC solar shield (model IR-SS, Campbell Scientific Ltd., Shepshed, UK). The IRTs were installed to aim vertically downward (nadir view) by targeting the center of the canopy from a distance of approximately 0.5 m over the targeted tree crown. The dense canopy of grapefruit trees, which areas ranged approximately between 7 to 9 m^2 depending on irrigation treatment, allowed the IRTs to view only foliage in a circular area of approximately 0.13 m^2 at the top of the canopy. Sensors were connected to dataloggers (model CR1000, Campbell Scientific Ltd., Shepshed, UK), which recorded the Tc every minute and stored the 15-min averages. The canopy temperature measurements began on 12 July, 2017 (DOY 212) and continued until 14 September (DOY 257). Air temperature (Ta) along with VPD data were recorded in the orchard every 15 min with a Campbell weather station (Campbell Scientific Ltd., Shepshed, UK).

Considering the Tc values obtained at the tree level, the following thermal indices were calculated: the difference between canopy and the surrounding air (Tc-Ta) and the crop water stress index (CWSI).

CWSI was calculated with empirical methodology as follows [21]:

$$CWSI = \frac{(Tc - Ta) - (Tc - Ta)_{LL}}{(Tc - Ta)_{UL} - (Tc - Ta)_{LL}} \quad (1)$$

where Tc-Ta denotes the measured canopy − air temperature difference. $(\text{Tc-Ta})_{\text{LL}}$ is the lower limit of (Tc-Ta) for a given vapor pressure deficit (VPD), which is equivalent to a canopy transpiring at the potential rate, and $(\text{Tc-Ta})_{\text{UL}}$ is the maximum (Tc-Ta), which corresponds to a canopy where transpiration is completely halted. The relationship between Tc-Ta and VPD for fully irrigated control trees from transfer water (TW-FI) was used to establish the Non Water Stressed Baseline (NWSB), which defines the lower limit $(\text{Tc-Ta})_{\text{LL}}$ for a given evaporative demand. Hence, $(\text{Tc-Ta})_{\text{LL}}$ is a linear function of VPD that, once empirically obtained, is calculated by solving the baseline equation (NWSB) for the actual VPD. $(\text{Tc-Ta})_{\text{UL}}$ is a fixed value related to Ta, as in Reference [36]. Specifically, in our experiment, UL was defined as Ta+4, which is a value adapted from lime [30] and from orange and mandarin [26]. From the entire season, only cloudless days from mid-July to mid-September were selected for the calculation of the CWSI. Only cloudless days were used for NWSB determination. Clear-sky days following a rainfall event were also discarded to avoid errors associated with wet foliage [27]. Depending on atmospheric, crop, and soil water conditions, it is occasionally possible to measure Tc values greater than the upper baseline. Therefore, CWSI can be slightly greater than 1 [37].

2.4. Experimental Design and Statistical Analysis

A total of 192 trees were used in this study. The experimental design of each irrigation treatment was 4 replicates distributed following a completely randomized design. Each replica consisted of 12 trees and organized into 3 adjacent rows. Two trees from the middle row from each replication were used for measurements and the rest acted as borders and were excluded from the study to eliminate potential border effects.

The coefficient of variations (C_v, the ratio of the standard deviation to the mean) of the canopy temperature measured by the IRTs was determined for each treatment.

A weighted analysis of variance (ANOVA) followed by Tukey's test ($P \leq 0.05$) was used for assessing differences among treatments. Linear regressions among the variables measured in the field and spectral data were calculated. Pearson´s correlation coefficients were used to assess the significance of these relationships. These statistical analyses were performed using SPSS (vers. 23.0 for Windows, SPSS Inc., Chicago, IL, USA). To discriminate significant differences among parameters of different linear regressions (slope and intercept), the analysis of covariance (ANCOVA) were performed using Statgraphics software (Statgraphics Plus for Windows Version 4.1).

3. Results

3.1. Climate Parameters and Analysis of Seasonal Tc Variability by IRT

The degree of variation in the temperature of the canopy (Tc) measured by infrared sensors (IRTs) among the trees from the same irrigation treatment is not generally known [3]. To characterize such variability, the coefficient of variations (C_v) of Tc was determined for each treatment. The C_v of the Tc readings from the different IRTs (measurements at 15 min intervals) were 0.38%, 0.56%, 0.55%, and 1.65% for TW-FI (transfer water − full irrigation), TW-RDI (transfer water − regulated deficit irrigation), RW-FI (reclaimed water − full irrigation), and RW-RDI (reclaimed water − regulated deficit irrigation), respectively. In RW-RDI, about 92.6% of the data showed a C_v of less than 5% and about

70% of the data of less than 2%. This high C_v was due to humidity problems inside the sensor on rainy days. For the calculation of the NWSB, these data were not taken into account. In the rest of the treatments, about 99.59%, 94.85%, and 96.30% of the total data had a C_v of less than 2%. Thus, the low C_v of Tc showed a little variation among trees of the same treatment. It also proved that the canopy surface viewed by the sensor (or the number of leaves falling inside the sensor field of view) was enough to remove the variability due to the leaves' orientation with respect to the sun angle.

3.2. Diurnal Course Patterns of Tc and Tc-Ta Oscillations by IRT

Figure 2 shows the hourly trend of Tc and solar radiation (Rs) (A, B, and C) and Tc-Ta and DPV (D, E, and F) for all treatments at three different moments of the RDI period including at the beginning (DOY 193, after 9 days with RDI), medium (DOY 224, after 40 days), and at the end (DOY 257, after 72 days) in order to understand the behavior of such parameters at different water stress levels.

In general, Tc showed large oscillations at around 12.00–16.00 GMT on DOY 193 and 257 and at 09.00–16.00 on DOY 224 when VPD was lower. The oscillations varied up to more than 1 °C in 30 min. The differences between the treatments increased as the day progressed and generally disappeared at around 18:00 (GMT) on DOY 193 and 257 and at 20.00 GMT on DOY 224, as a result of the decline in evaporative demand and in Rs. The highest differences in Tc among treatments were noticeably detected in the readings taken between 12.00 and 17.00 GMT. At the beginning of the RDI period (DOY 193), the treatments did not show significant Tc differences since the RDI treatments had been only subjected to a week of deficit irrigation (Figure 2A). At medium and final RDI periods (DOYs 224 and 257), the differences between the control and stressed trees became significant (Figure 2B,C). The maximum difference between the canopy temperatures of the treatments was 6.85 °C, recorded on DOY 256 for RW-RDI with respect to TW-FI, four days before the end of the RDI stress period (data not shown).

The Tc values were higher than the air temperature (Ta) approximately from 5.00 GMT to 18.00 GMT (the canopy being warmer than the air) and, thus, the values of the Tc-Ta difference were above 0 °C. Nevertheless, in the evening and at night, sometimes the Tc-Ta values became negative in all treatments (Figure 2D–F) although the fully irrigated canopies were cooler than those of the stress treatments and, consequently, their Tc-Ta values were the most negative. The daily Tc-Ta averages were 0.71, 0.79, 0.96 and 1.01 °C for TW-FI, TW-RDI, RW-FI, and RW-RDI, respectively. Thus, RDI and RW treatments had higher $Tc-Ta$ values than control trees during the period of experimentation. In all the treatments, the maximum values of Tc-Ta were reached before and after the peaks of VPD and Rs, respectively. The RW-RDI treatment showed the maximum Tc-Ta registered during the experiment (7.65 °C on DOY 211) (data not shown) 37 days after the beginning of the RDI period, which coincides with a day of high VPD.

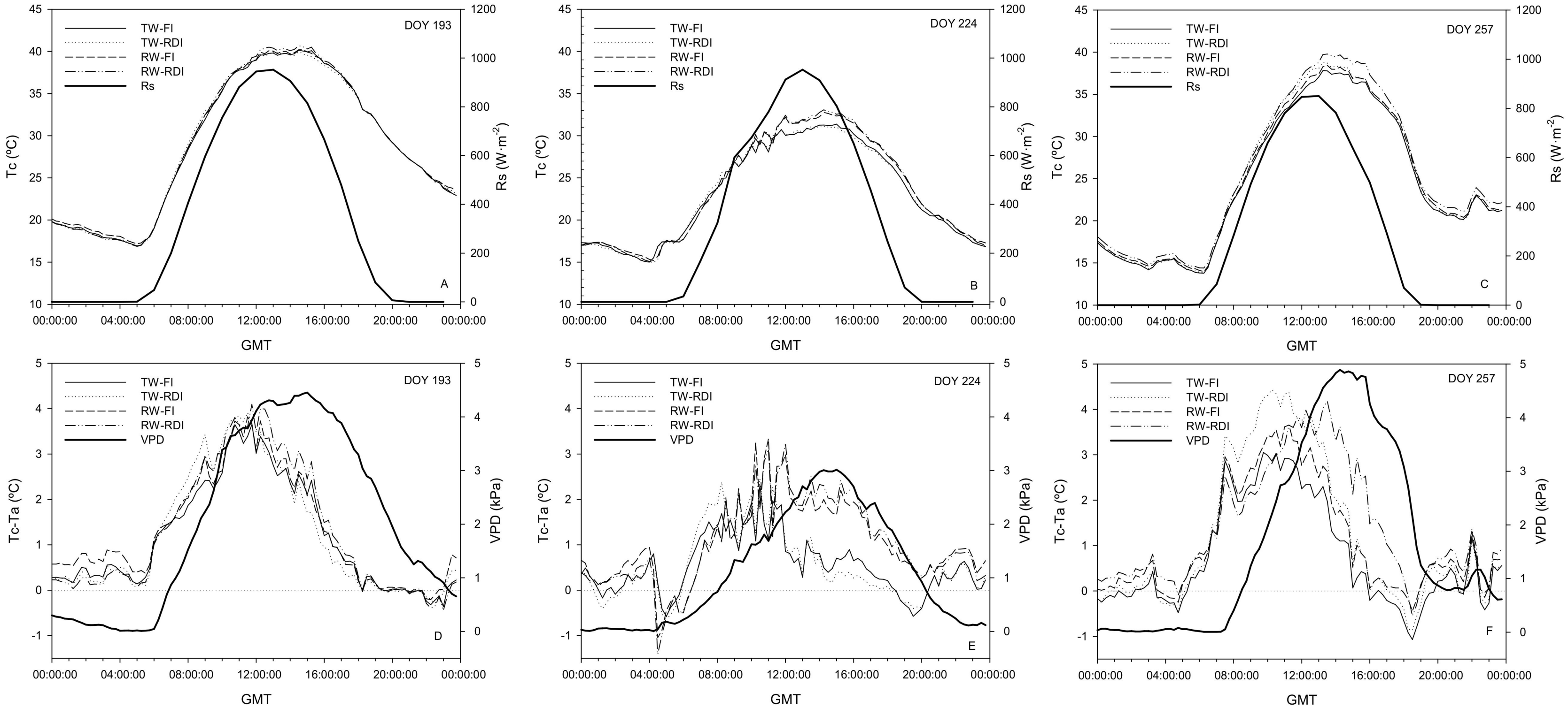

Figure 2. Representative diurnal course patterns of canopy temperature, Tc (°C) and evolution of solar radiation, Rs ($W \cdot m^{-2}$) (top row: (**A–C**)) and representative diurnal course patterns of Tc-Ta (°C) and evolution of VPD (kPa) (bottom row: (**D**–**F**)) for each treatment: TW-FI (transfer water-full irrigation), TW-RDI (transfer water-regulated deficit irrigation), RW-FI (reclaimed water-full irrigation) and RW-RDI (reclaimed water-regulated deficit irrigation) on three days that differed in tree water status: DOY 193, 224, and 257 in 2017. Each Tc reading corresponded to the averaged value from four trees of the same treatment.

3.3. Establishment of the Non-Water Stressed Baseline (NWSB) with Tc Measured by Thermometry

The first attempt for obtaining the non-water stressed baseline (NWSB) pooled together Tc-Ta and VPD data from all hours and cloudless days of the full irrigated trees with TW, but the data yielded was too scattered, which makes it impossible to obtain a reasonably $(Tc\text{-}Ta)_{LL}$ (data not shown).

To accurately define the NWSB, we assessed the data in different ways. First, in order to find the optimum time interval for the NWSB establishment, we averaged the Tc-Ta values over different time intervals, ranging from 30–45–60 min. It is convenient to remember the Tc readings were collected by IRTs every 15 min. The best adjustment was shown for 60-min Tc-Ta averages. In Figure 3, the two linear regressions obtained for fully irrigated trees (TW-FI) at 08.00 GMT are shown as an example. Tests carried out in the remaining datasets displayed very similar results. Thus, for all the subsequent thermometry analyses, 60-min Tc-Ta and VPD averages were utilized.

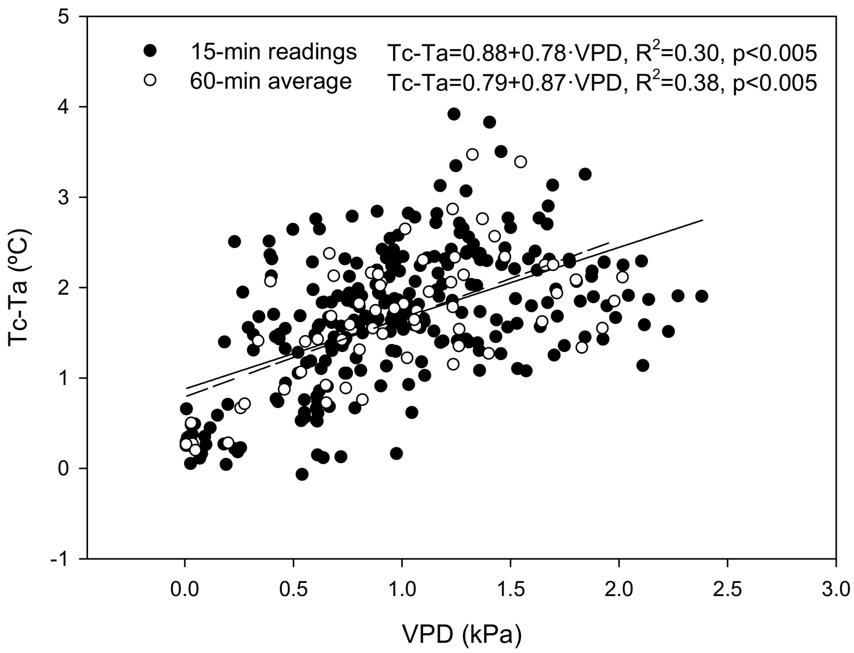

Figure 3. Example of relationship between Tc-Ta (°C) and VPD (kPa), using 15-min readings and 60-min averaged obtained at 8.00 GMT for full-irrigated trees (TW-FI) during the experimental period in 2017. Solid line and dash line correspond to linear regressions for 15-min readings and for 60-min average, respectively.

Then, the NWSBs for the different hours of the day were determined. The relationships Tc-Ta versus VPD were significant ($p < 0.005$) for each hour, as shown in Table 2. However, the data scattering was large. We found marked changes in the NWSB parameters over the diurnal-course. The coefficients of correlation displayed moderate values, ranging between 0.72–0.38 and were notably affected by the period of daytime. The highest R value was found early in the morning (R = 0.72 at 08.00 GMT) and gradually decreased down to 0.38 at 17.00 GMT. The slope and intercepts of the fitted NWSBs also varied throughout the day. The slopes progressively decreased from +1.12 $°C\cdot kPa^{-1}$ at 08.00 GMT to +0.14 $°C\cdot kPa^{-1}$ at 17.00 GMT. The intercept showed a similar trend even though it was less linear with a maximum value of +0.61 °C at 08.00 GMT and a minimum value of +0.08 °C at 17.00 GMT. It can be observed that both fitted parameters decreased about 8 times over time. The maximum Tc-Ta values were collected before the VPD and zenith solar angle (θZ) reached their maximum and minimum values, respectively (Table 2).

Table 2. Significant hourly correlations between Tc-Ta versus VPD using cloudless days of year (DOY) 193–257 for the non-water stressed baseline (NSWB). GMT: Greenwich Mean Time. VPD: Vapor pressure deficit. θZ: zenith solar angle. The suffix $_{av}$ indicates the average. Each value is obtained from hourly Tc-Ta and VPD average in a given day at a given hour, using the Tc of the fully irrigated trees (TW-FI). Number of points for each regression was 53. Different letters within the same column indicate significant differences among Time (GMT), according to ANCOVA ($P < 0.01$).

Time (GMT)	Slope (°C·kPa^{-1})	Intercept (°C)	R	*P*	VPD$_{av}$ (kPa)	(Tc-Ta)$_{av}$ (°C)	θZ (°)
08.00	1.12a	0.61a	0.72	<0.005	1.00	1.64	59.79
09.00	0.84ab	0.54bc	0.71	<0.005	1.53	1.83	48.32
10.00	0.74bc	0.61c	0.70	<0.005	1.96	2.04	37.64
11.00	0.54bcd	0.56d	0.55	<0.005	2.36	1.90	28.90
12.00	0.44de	0.44ef	0.52	<0.005	2.70	1.73	24.54
13.00	0.38ef	0.36f	0.49	<0.005	2.93	1.47	27.08
14.00	0.32efg	0.22gh	0.47	<0.005	2.93	1.14	34.96
15.00	0.23fg	0.28h	0.34	<0.005	2.79	0.92	45.32
16.00	0.21fg	0.11i	0.40	<0.005	2.55	0.62	56.69
17.00	0.14g	0.08j	0.38	<0.005	2.16	0.32	68.42

To study if there was a seasonal effect on the data, in addition to the hourly effect on fitted parameters of the NWSBs observed in Table 2, the period of the experiment from DOY 193 to 257 was divided into 3 groups based on solar radiation and VPD levels. Period 1 (P1) was comprised from DOY 193 to 212. Period 2 (P2) was comprised from DOY 213 to 239 and Period 3 (P3) was comprised from DOY 240 to 257. The parameters of the baseline equations obtained at different times and periods are given in Table 3.

Table 3. Hourly correlations between Tc-Ta versus VPD to establish non-water stressed baselines (NSWBs) using cloudless days for different seasonal periods. Period 1 (P1, DOY 193 to 212), period 2 (P2, DOY 213 to 239), and period 3 (P3, DOY 240 to 257). GMT: Greenwich Mean Time. VPD: Vapor pressure deficit. Rs: Solar radiation. The suffix $_{av}$ indicate the average. Each value is obtained from hourly Tc-Ta and VPD average at a given hour of a given day of each period, using the Tc of the fully irrigated trees (TW-FI). Number of points for each regression was 19, 19, and 15 for P1, P2, and P3, respectively. Different letters within the same column indicate significant differences among Time (GMT), according to ANCOVA ($P < 0.01$).

Time (GMT)	P	Slope (°C·kPa^{-1})	Intercept (°C)	R	*P*	VPD$_{av}$ (kPa)	(Tc-Ta)$_{av}$ (°C)	Rs$_{av}$ (W·m^{-2})
08.00	1	0.90a	0.99a	0.54	<0.01	1.33	1.94	332.99
	2	1.01a	0.56b	0.59	<0.005	0.67	1.38	278.67
	3	0.68a	0.63b	0.64	<0.005	1.24	1.60	195.51
09.00	1	0.60a	1.28a	0.62	<0.005	1.94	2.06	540.70
	2	0.61a	0.57b	0.57	<0.005	1.12	1.56	454.63
	3	0.72a	1.02a	0.51	<0.01	1.93	2.25	360.44
10.00	1	0.53a	1.27a	0.73	<0.005	2.40	2.25	698.79
	2	0.50a	0.71b	0.54	<0.005	1.51	1.79	604.76
	3	0.78a	0.97a	0.62	<0.005	2.38	2.41	520.61

Table 3. *Cont.*

Time (GMT)	P	Slope (°C·kPa^{-1})	Intercept (°C)	R	*P*	VPD_{av} (kPa)	$(Tc\text{-}Ta)_{av}$ (°C)	Rs_{av} (W·m^{-2})
11.00	1	0.32a	1.52a	0.52	<0.01	2.81	2.16	816.05
	2	0.44a	0.31b	0.76	<0.005	1.90	1.62	717.18
	3	0.61a	0.77a	0.60	<0.005	2.76	2.20	627.74
12.00	1	0.11a	2.12a	0.25	ns	3.22	2.14	896.00
	2	0.31ab	0.27b	0.72	<0.005	2.20	1.32	795.53
	3	0.55b	0.46c	0.78	<0.005	3.06	2.00	706.34
13.00	1	−0.03a	2.41a	0.06	ns	3.48	1.96	925.11
	2	0.37b	0.20b	0.75	<0.005	2.39	1.00	841.71
	3	0.38b	0.48c	0.71	<0.005	3.27	1.78	686.48
14.00	1	0.02a	1.87a	0.05	ns	3.46	1.57	885.50
	2	0.18a	0.11b	0.54	<0.005	2.41	0.75	796.73
	3	0.24a	0.46c	0.69	<0.005	3.37	1.27	647.08
15.00	1	0.04a	1.45a	0.14	ns	3.22	1.31	772.09
	2	0.20ab	0.08b	0.62	<0.005	2.31	0.62	679.19
	3	−0.10b	1.09c	0.47	<0.025	3.35	0.75	584.91
16.00	1	−0.13a	1.55a	0.52	<0.01	3.01	0.94	637.68
	2	0.14b	0.05b	0.46	<0.01	2.08	0.38	533.90
	3	−0.19a	0.91c	0.77	<0.005	3.01	0.37	463.22
17.00	1	−0.10ab	0.96a	0.39	<0.05	2.59	0.55	456.58
	2	−0.07b	0.03b	0.35	<0.05	1.72	0.17	347.53
	3	−0.20a	0.51c	0.84	<0.005	2.65	0.03	261.59

When Tc-Ta and VPD were plotted for a given hour of the day and a given period (Table 3), the hourly effect on the coefficients of correlation across periods was not observed (Table 2). The R did not improve in the early hours of the day (08.00–9.00 GMT). However, it increased significantly when Tc-Ta and VPD were regressed for the middle hours of the day, from 11.00 to 16.00 GMT, in P2 and P3, which showed lower solar radiation than P1 (a good correlation was found between Tc-Ta and Rs data from Table 3: Rs = 168.26·Tc-Ta + 193.91, $R^2 = 0.41$, $p < 0.005$). For the rest of the hours (10.00 and 16.00–17.00 GMT), the level of agreement also improved in P1 and P3, showing values of VPD and Tc-Ta higher than the values of P2.

The NWSB-slopes progressively decreased during the diurnal time-course in general, as shown in Table 3. In the afternoon, some slopes became negative, mainly during P3. In addition, the slopes values were lower than in Table 2 except between 10.00–12.00 GMT for P3 when the slope was the steepest.

As for the NWSB-intercepts, for P1 and P3, the values were higher than when all the days were plotted together (Table 3). The intercepts from P2 did not increase, as the Tc-Ta levels were lower than the others periods of study. An example of how the lower Tc-Ta the lower VPD and NWSB-intercept, as in P2, is depicted in Figure 4.

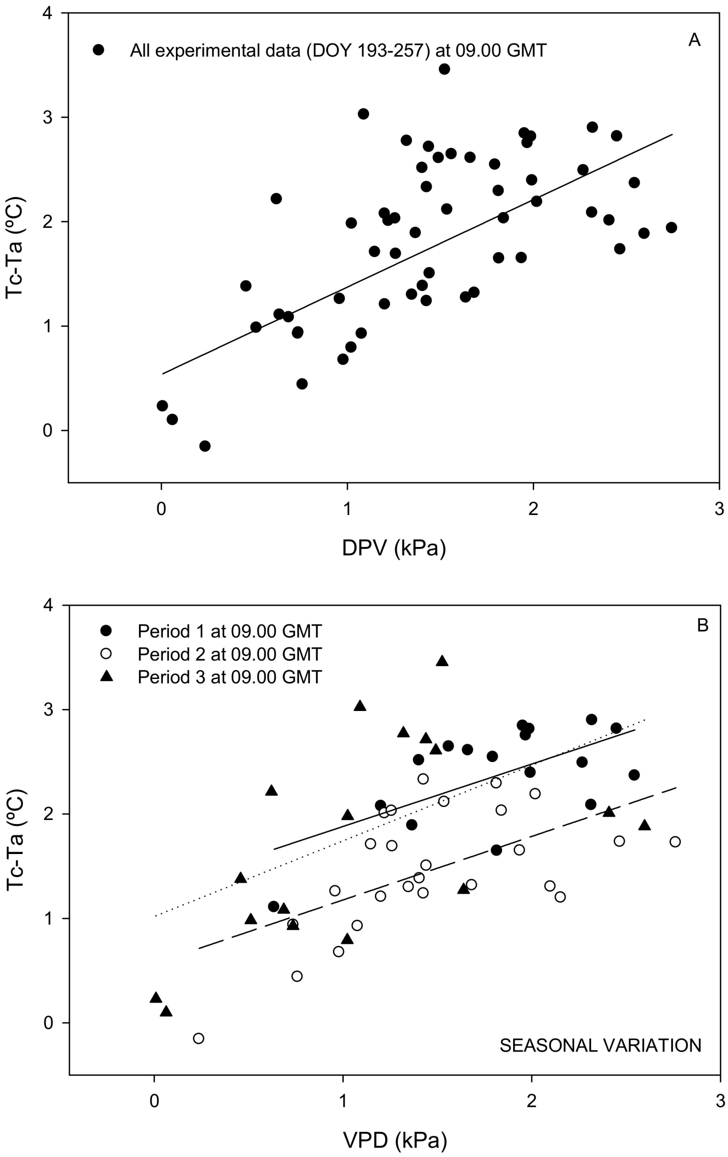

Figure 4. Seasonal variation of non-water stress baselines (NWSBs). Relationships between Tc-Ta (C°) and VPD (kPa) with (**A**) data from the experimental period (DOY 193-257) plotted together at 09.00 GMT and (**B**) data split into three different periods: 1 (P1, DOY 193-212), 2 (P2, DOY 213-239), and 3 (P3, DOY 240-257). Only clear-sky and non-rainy days were used in the calculations. The linear regressions are shown in Tables 2 and 3. The solid line, long dash line, and dotted line correspond to linear regressions for P1, P2, and P3, respectively.

In addition, unlike the data shown in Table 2, the values of the intercepts increased until a given moment of the day and then decreased, mainly in P1 (maximum values of the intercepts were 2.41 at 13.00 GMT in P1, 0.71 at 10.00 GMT in P2, and 1.02 at 09.00 GMT in P3) (Table 3). Thus, the lowest values of the intercepts were found in the early morning and afternoon. We found a significant negative correlation between intercept values and the respective correlation coefficients of P1, P2, and P3 (Intercept (°C) = $-1.78 \cdot R + 1.85$, $R^2 = 0.35$, $p < 0.005$). Therefore, the linear regressions Tc-Ta versus VPD had a better correlation coefficient when the NWSB-intercept parameter was smaller.

Moreover, the NWSBs derived during the three periods of study also displayed a strong hourly variation, which can be observed in the example shown in Figure 5. NWSB-slopes were successfully modeled for the diurnal time-course with linear regressions (Figure 6).

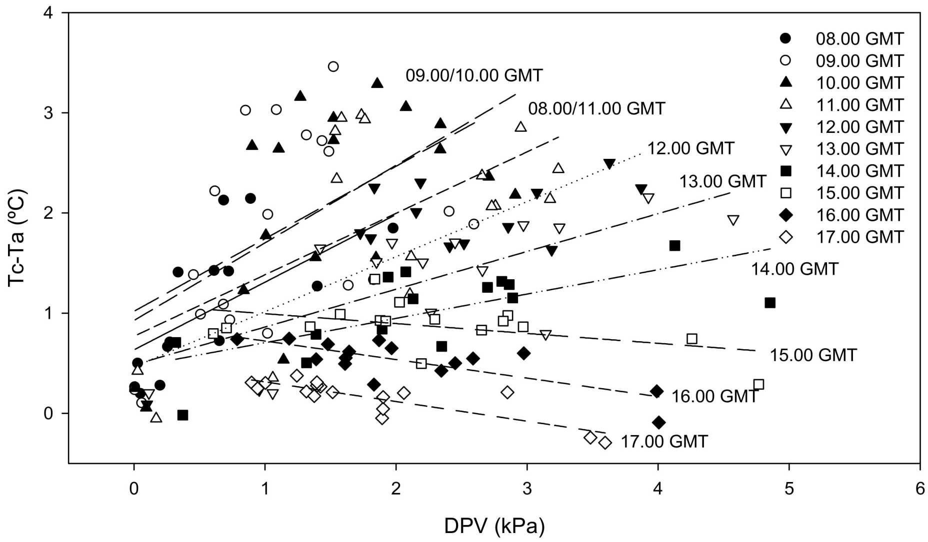

Figure 5. Hourly variation of non-water stress baselines (NWSBs). Relationships between Tc-Ta (C°) and VPD (kPa) with data from fully irrigated trees (TW-FI) in Period 3 (P3, DOY 240-257) from 08.00-17.00 GMT. Only clear-sky and non-rainy days were used in the calculations. The linear regressions are shown in Table 3.

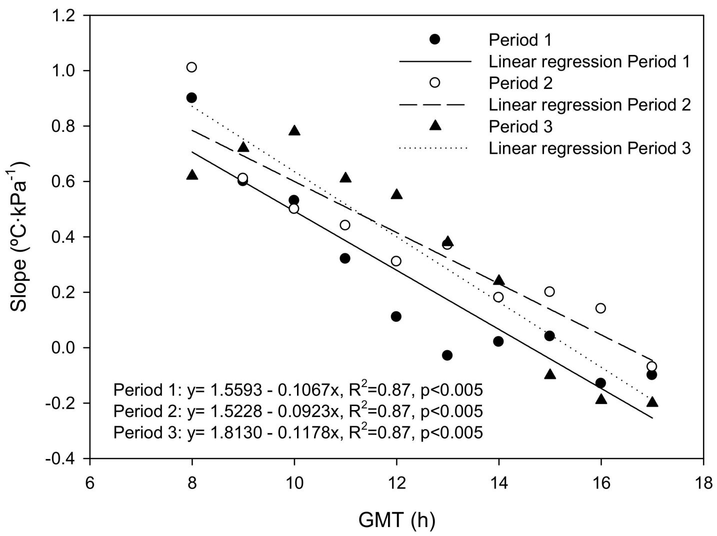

Figure 6. Best-fit to the NWSB-slope for the three periods: 1 (P1, DOY 193-212), 2 (P2, DOY 213-239), and 3 (P3, DOY 240-257).

In order to verify whether this hourly variation was related with Rs, we plotted the parameters of the equations of the NWSBs obtained for the different periods against the θZ [16,27] (Figure 7). The correlation between the NWSB-intercepts and θZ was significant (R^2 = 0.37, p < 0.005). At midday, when the θZ was closer to 0, the intercepts were greater (Figure 7A). The NWSB-slopes were also well correlated with θZ. As depicted in Figure 7B, this relationship showed a marked hysteresis. Until noon (08.00–12.00 GMT), the slopes were positive and increased with θZ (R^2 = 0.73, p < 0.005). However, from the early afternoon (13.00–17.00 GMT), the slopes were negative and decreased as the solar angle increased (R^2 = 0.56, p < 0.005). The θZ was also significantly negatively correlated with the difference Tc-Ta (Tc-Ta (°C) = −0.03 · θZ (°) + 2.56, R = 0.58, p < 0.005). The higher the zenith angle is, the smaller the difference in Tc-Ta is.

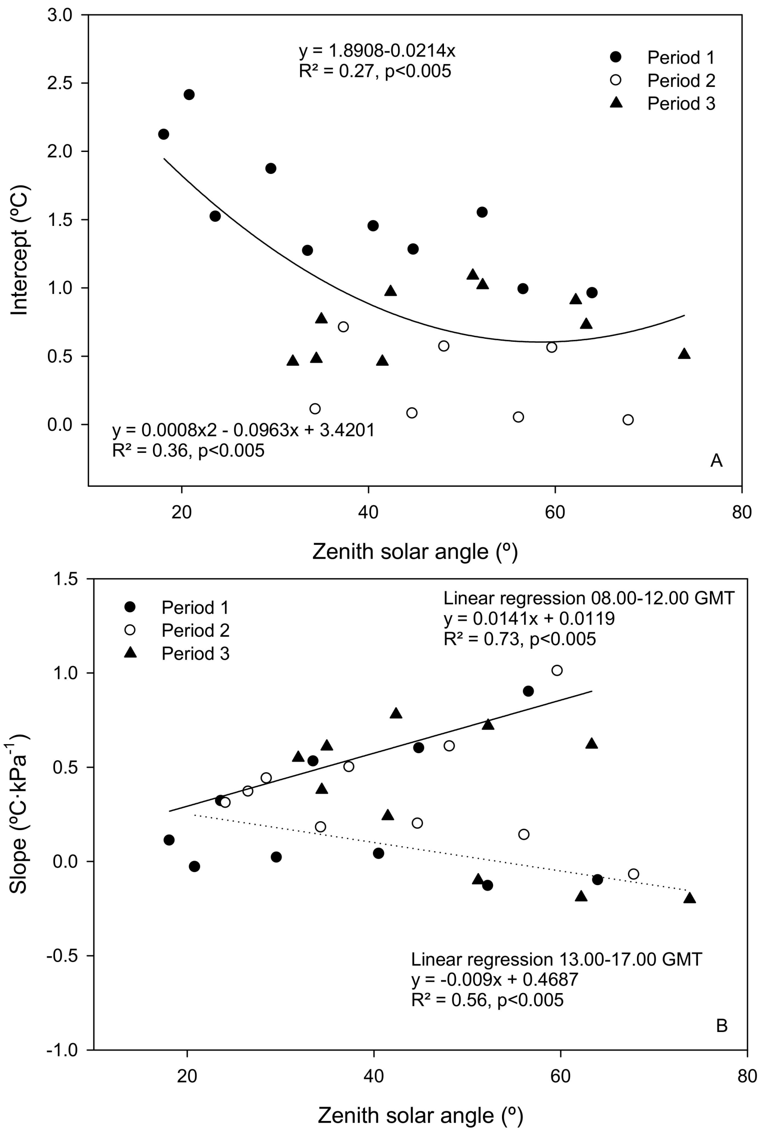

Figure 7. Relationships of zenith solar angle (θZ) with (**A**) NWSB-intercepts and (**B**) NWSB-slopes for the three different periods: 1 (P1, DOY 193-212), 2 (P2, DOY 213-239), and 3 (P3, DOY 240-257).

3.4. Seasonal Evolution and Correlations between Thermal Indicators (Tc, Tc-Ta, CWSI) Obtained by Thermometry and Water Relations (Ψ_{stem})

CWSI was calculated at 10.00 GMT since the differences Tc-Ta were the highest at this moment. The NSWBs obtained at 10.00 GMT for each period were used, since they had good correlation coefficients ($p < 0.005$) (0.73, 0.54 and 0.63 for P1, P2, and P3, respectively, Table 3) and presented the highest Tc-Ta values.

The three NWSBs with negative slopes found at 17.00 (Table 3) can also be used for the calculation of CWSI given that results were comparatively similar to those obtained when the CWSI was calculated with the NWSBs at 10.00 GMT. The only difference was that the values of all the treatments were slightly higher and further from 0 when the CWSI was calculated with the negative NWSBs than with those obtained at 10.00 GMT.

In order to define the most advisable thermal indicator for estimating the water status of grapefruit plants irrigated with RW and RDI, we assessed the thermal information and the water potential throughout the experimental period. Figures 8 and 9 show the evolution of Tc, Tc-Ta, CWSI, and stem water potential for all the treatments.

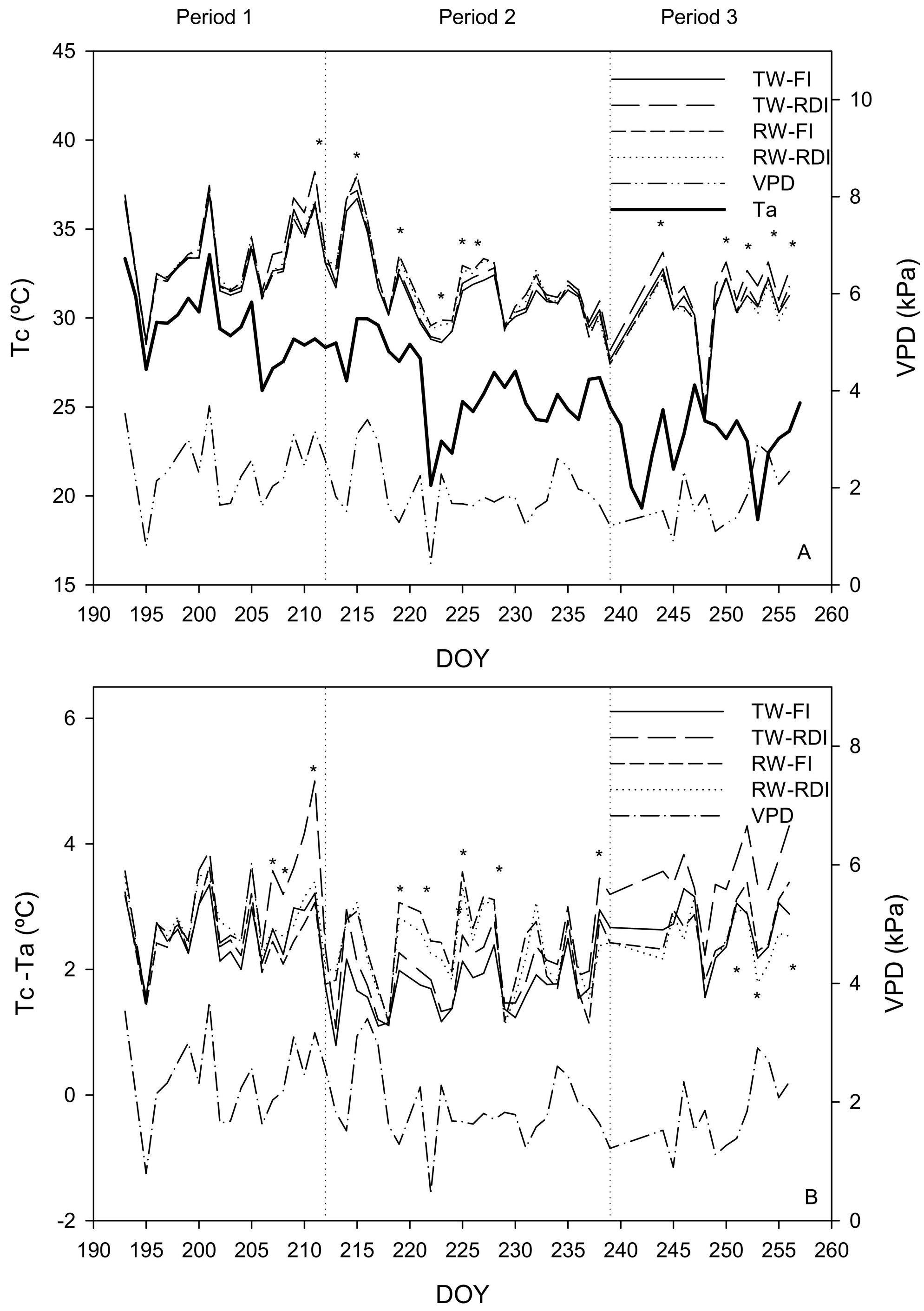

Figure 8. Evolution of (**A**) temperature of canopy (Tc, °C), (**B**) difference between Tc-Ta (Tc-Ta, °C), (C) crop water stress index (CWSI) collected at 10.00 GMT and (D) stem water potential (Ψ_{stem}, MPa) for each treatment: TW-FI (transfer water-full irrigation), TW-RDI (transfer water-regulated deficit irrigation), RW-FI (reclaimed water-full irrigation), and RW-RDI (reclaimed water-regulated deficit irrigation) during the experimental period. Each value is the average of four individual measurements per tree and replicate. * Indicates significant differences among treatments, according to Tukey's test ($P < 0.05$). The discontinuous vertical lines divide the experimental period into three periods with a different water stress level: 1 (DOY 193-212), 2 (DOY 213-239), and 3 (DOY 240-257).

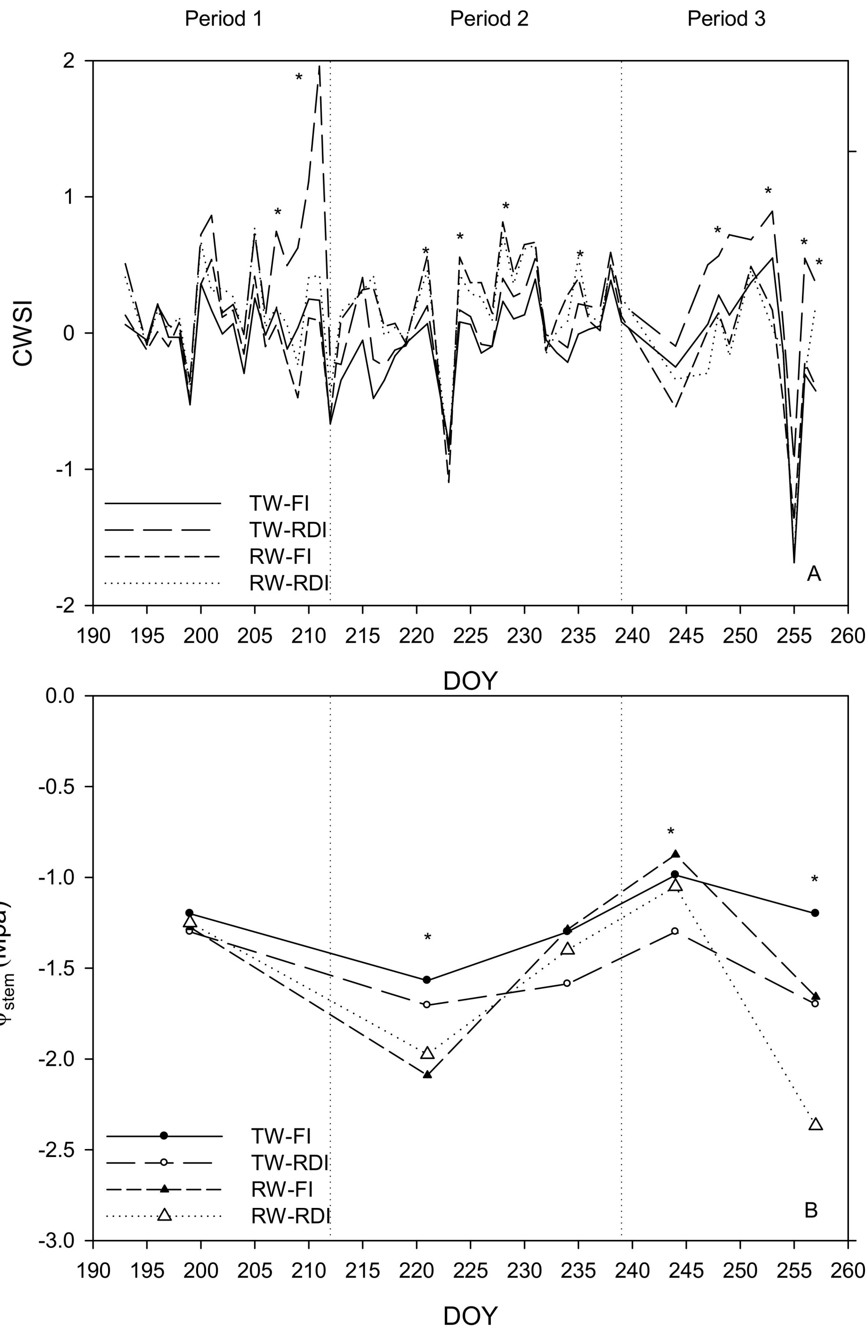

Figure 9. Evolution of (**A**) crop water stress index (CWSI) collected at 10.00 GMT and (**B**) stem water potential (Ψ_{stem}, MPa) for each treatment: TW-FI (transfer water-full irrigation), TW-RDI (transfer water-regulated deficit irrigation), RW-FI (reclaimed water-full irrigation), and RW-RDI (reclaimed water-regulated deficit irrigation) during the experimental period. Each value is the average of four individual measurements per tree and replicate. * Indicates significant differences among treatments, according to Tukey's test ($P < 0.05$). The discontinuous vertical lines divide the experimental period into three periods with a different water stress level: 1 (DOY 193-212), 2 (DOY 213-239), and 3 (DOY 240-257).

Tc was influenced largely by VPD (Figure 8A). In P1, the average values at 10.00 GMT were 33.23, 33.75, 33.20, and 33.45 °C for TW-FI, TW-RDI, RW-FI, and RW-RDI, respectively. TW-RDI had significantly higher levels than the rest of the trees, reaching maximums of up to 39.28 °C. In P2, the Tc decreased (31.39, 31.68, 32.03, and 31.99 °C for TW-FI, TW-RDI, RW-FI, and RW-RDI, respectively) with respect to P1, and the RW treatments had a maximum value of 39.19 °C, which was significantly higher than the control trees for several days. In P3, the Tc decreased again (30.13, 30.87, 30.09, and 29.95 °C for TW-FI, TW-RDI, RW-FI, and RW-RDI, respectively) and TW-RDI had significant values (35.03 °C) that were higher than the rest of the treatments.

The same trend for the seasonal course of Tc-Ta was observed even though Tc-Ta values in P3 were higher than in P2 because Ta decreased to a greater degree than Tc (Figure 8B). In general, the fully irrigated canopies were cooler and, consequently, Tc-Ta was more negative than in the rest of stress treatments, except in RW-RDI trees in P3. This treatment showed their maximum values of Tc-Ta at 12.00 GMT and, therefore, the Tc-Ta collected at 10.00 GMT were lower than those found in control trees (Figure 8B).

The seasonal pattern of the CWSI for all treatments can be observed in Figure 9A. It is important to highlight that the most accurate CWSI data were found at 10.00 GMT for all the treatments since, at that time, the Tc-Ta reached the highest values, except for RW-RDI in P3. For this reason, the CWSI from RW-RDI in the last period was calculated at 12.00 GMT. In this way, the results were markedly influenced by the irrigation regime (Figure 9A). In control trees, CWSI values were close to 0 for the whole season, with a mean value of 0.00, −0.05, and 0.14 for P1, P2, and P3, respectively. During the initial water stress period (DOY 193-212), the deficit irrigation treatments, mainly TW-RDI, exhibited CWSI values that were higher than those found in control trees, up to approximately 0.41 on average. During the middle water stress period (DOY 213-239), the highest CWSI was found in RW treatments (0.24 and 0.22 on average). In the last water stress period (DOY 240-257), TW-RDI was the treatment with the uppermost CWSI.

The major differences between CWSI from control trees and the different stress treatments were for TW-RDI in P1 and P3 (0.41 and 0.43, respectively), for RW-FI in P2 (0.30), and for RW -RDI in P3 (0.28).

Another important aspect to be noted is that there were some days of unreasonable CWSI, with values well above 1 or well below 0, namely DOY 211 and 255. These days were characterized by Ta and/or VPD below or above of the average, i.e., with a different atmospheric environment from the period used to derive the NWSB. Under these conditions, $(\text{Tc-Ta})_{LL}$ is usually too high or too low compared to the Tc. Thus, the CWSI is unreliable and the signal-to-noise ratio of the CWSI is worse [12,16].

The measurements of Ψ_{stem} showed the seasonal evolution of the water stress in the treatments (Figure 9B). During most of the experimental period, control trees had an average value of around −1.18 MPa, which is indicative of a near-optimum plant water status [10,38]. The RDI treatments decreased to −1.75 and −2.4 MPa for TW-RDI and RW-RDI, respectively, at the end of the RDI period, which indicated that plant water stress experienced by RDI trees was moderately severe, according to the CWSI results. RW-FI also showed values close to −2 MPa in P2. Rainfall events occurred during this period on DOYs 241 and 242, which resulted in a temporary recovery of water deficit at the beginning of P3 (Figure 9B). Thus, the plant water status of the treatments was not exclusively a consequence of the differential irrigation treatments applied.

The thermal indicators (Tc, Tc-Ta, and CWSI) derived from thermometry for all the treatments were plotted against the stem water potential. Significant linear regressions were observed in all cases (Table 4) and the goodness-of-fit of the relationship were similar ($p < 0.005$) even though CWSI versus Ψ_{stem} had the highest correlation coefficient. The relationship between CWSI and Tc-Ta was somewhat weaker ($p < 0.01$) than previously described (Table 4). When the thermal indicators were plotted against Ψ_{stem} for each treatment (TW-FI, TW-RDI, RW-FI, and RW-RDI), the linear regressions were also significant, but to a lesser degree ($p < 0.05$).

These good correlations were corroborated in DOY 257, when the RDI trees were near the end of the deficit irrigation period and, thus, quite stressed, as shown by the leaf water potential data shown in Figure 8D. While the CWSI of the control trees was near zero, the CWSI of the RW and RDI trees was higher and the Ψ_{stem} significantly lower, which was likely a result of a decrease in the canopy conductance of the RDI trees in response to water [16] and saline stress.

Table 4. Correlation coefficients (R) for linear regression, slope (a), and intercept (b) found between stem water potential (Ψ_{stem}) versus canopy temperature (Tc), difference between canopy and air temperature (Tc-Ta), and crop water stress index (CWSI) and CWSI versus Tc-Ta of grapefruits trees, regardless of irrigation treatments, during the RDI period (from DOY 193 to 257). N = 20 (average value of each treatment and five days).

	Slope (a)	Intercept (b)	R	*P*
Tc versus Ψ_{stem}	−0.15	3.56	0.57	<0.005
Tc-Ta versus Ψ_{stem}	−0.33	−0.64	0.63	<0.005
CWSI versus Ψ_{stem}	−0.65	−1.47	0.74	<0.005
CWSI versus Tc-Ta	+0.97	2.41	0.51	<0.01

4. Discussion

The data of the canopy temperature measured by thermometry (IRT) between trees of the same treatment showed a low variability, which suggests that observed trees were in a similar water status and the sensors were properly positioned to remove the variability due to the leaves' orientation with respect to the solar angle [16].

The canopy temperature and vapor pressure deficit followed a diurnal curve that was largely influenced by the solar radiation cycle (Figure 2). On a typical summer day, evaporative demand increases as the day advances. The transpiration rate and stomatal aperture would increase too, which would lead to cooler canopies [3] in fruit trees. However, this stomatal response to environmental conditions varies among species [23]. Citrus show a conservative behavior. The increase of temperature throughout the day of grapefruit trees implies a partial stomatal closure that results in a low transpiration rate [11], even under full irrigation conditions [3,10] and a low VPD as well. The maximum stomatal aperture is reached in the early morning and then the stomata are partially closed for the rest of the day [10]. This characteristic of citrus groves is well known and has been characterized in the past [26,39,40]. In addition, transpiration in citrus is less than that of other fruit tree species during the summer [41]. This information the daily patterns of stomatal closure of grapefruit trees is key for understanding fluctuation of the canopy.

In our study, Tc was higher than Ta in full irrigation and water and saline stress conditions during the middle hours of the day, which results in positive values of Tc-Ta for a wide range of VPD, as reported [26] for orange and mandarin trees. On the contrary, other authors found that Tc was lower than Ta in sweet lime, which gives negative Tc-Ta values. This could be explained since the water use of sweet lime is quite different from other citrus species [30].

The major Tc-Ta value was observed before 12.000 GMT for all treatments (Figure 2), which indicates the maximum amount of differential stress throughout the day and justifies the use of measurements to represent indices such as CWSI. At night, the canopy temperatures converged [37] and the Tc-Ta difference of all trees approached 0 °C, which is slightly higher for RW and RDI treatments.

During the period of experimentation, the treatments showed clear differences in Tc, mainly in the middle and final stages of RDI, which indicates the dependence of canopy temperature on salinity and deficit irrigation. This behavior could be symptomatic of reduced transpiration due to saline and water stresses. The maximum differences between the canopy temperatures of the treatments were recorded at the end of the RDI period for the treatment that combined both water and saline stresses. This maximum value (6.85 °C) was higher than others reported by References [22–24].

Establishing proper NWSBs is key for obtaining accurate CWSI values. The wide fluctuations observed in Tc (Figure 1) and the stomata closure suffered by citrus with the increase of the VPD [11] resulted in a laborious computation of the relationship between Tc-Ta versus VPD. Even though linear regressions representing the NWSB with a high significance ($p < 0.005$) were found, the scattering in the Tc-Ta difference versus VPD plots was large and was in agreement with other results obtained in citrus [26]. On the contrary, other crops where the NWSB was assessed, such as pistachio [16] or olive trees [27], presented less scattering than our data. This was likely due to the fluctuations in canopy temperature [26] that required the cautious evaluation of the time interval needed to estimate the mean canopy temperature in relation to the air temperature, as described in Figure 2. The best adjustment was shown for 60-min Tc-Ta averages, according to the data shown in other studies [26].

The best correlations between Tc-Ta and VPD were found in the early morning hours with low VPD and high Tc-Ta values (Table 1 and Figure 2). The slopes were positive since, when the VPD increases, stomata partially close, leaf temperature rises, and, hence, Tc-Ta increases [3]. Citrus are known to be conservative in water use and the stomatal conductance of citrus decreases with increasing vapor pressure deficits [11,42].

The NWSBs obtained in this case were not similar to that reported for the three other citrus crops in which the NWSBs have been published: sweet lime [43], orange, and mandarin [26]. So far, NWSB with a positive slope has not been reported based on our knowledge. In the two works cited above, Tc was generally higher than Ta for the usual values of VPD such as in grapefruit trees. However, the NWSB-slopes correlating Tc-Ta versus VPD were always negative, contrary to the slope found in our results. These differences can be explained in the case of sweet lime because the Tc was measured with a hand-held infrared thermometer 2 m away from the tree, around 15° above the horizontal, which is a procedure that would not assess the Tc of the top of the canopy. In the case of mandarin and orange trees, NWSBs were established using measurements of Tc-Ta averaged between 11:30 and 12:30 GMT of complete vegetative cycles: Tc-Ta = −0.50·VPD + 4.06 and Tc-Ta = −0.38·VPD + 4.59 for mandarin and orange, respectively.

The hourly variation found in the NWSBs has been described in three more crops, such as pistachio [16], grapevine [44] and olive [27], but it had not been described in citrus. These hourly changes were due to variations in all fitted parameters of the NWSB since both the slope and the intercept varied throughout the day. An explanation for the shifting of the NWSB was provided by Jackson's theoretical equation for the NWSB (Jackson et al. 1981), which showed that the intercept increases with Rs and decreases with wind speed. Such behavior was predicted theoretically by Reference [45], and supported with some measurements, but it has only been confirmed so far by Reference [16] for pistachio and Reference [27] for olive trees. In our study, IRTs were arranged in a nadir-view configuration, so they targeted a relatively horizontal foliage surface at the top of the canopy. The radiation incident over the canopy portion enclosed in the IRT field of view should be closely related to the solar angle [16]. The wind in the experimental zone of this study was moderate and constant throughout the test period. Thus, its effect on NWSB was negligible [16]. The NWSB-slope and intercept found was likely correlated with θZ ($p < 0.005$) (Figure 7). Regarding the NWSB-slope, it presented a marked hysteresis over the course day and it increased until midday and decreased from the early afternoon with θZ. As for the NWSB-intercept, it increased as the θZ approached 0° (at midday). In other studies, the relationships between intercept and solar radiation have been linear [16] or have shown a hysteresis during different seasonal periods [27]. As far as we know, it is the first time that relationships between the slope and the solar angle have been found.

Little is known about the seasonal variation in the NWSB, since, in most works, the baseline of a given species appears to be a very stable plant property. Nevertheless, Reference [27] found a seasonal effect during the growth cycle of olive trees and [18] reported small seasonal differences in peach trees. We divided the whole experimental period into three subperiods based on accumulated solar radiation and VPD. The level of agreement of the NWSBs improved during certain hours of the day and periods. Additionally, the intercept was greater in P1 and P3 (corresponding to the months of July and September) than in P2 (August) given that the Tc-Ta values were higher. In addition, we discovered that the smaller the intercept value was, the better correlations between Tc-Ta and VPD were. Lastly, when evaluating the data separately according to the different periods, we also found that the NWSB-slope became significantly negative in the afternoon.

The slope values were more influenced by the hour than seasonal variations and the intercept values by both. The hourly behavior changed significantly with the season (Figures 5 and 6).

The variation of the NWSBs raises the question of how the resulting CWSI changes when it is determined at different times of the day. In the past, many difficulties were encountered for the evaluation of CWSI in citrus [22] due to diurnal fluctuations in stomatal resistance [46] and in canopy conductance [47]. We found good NWSBs for different times of the day and different seasonal periods that were used for the calculation of accurate CWSI.

In addition to achieving accurate NWSBs, for an adequate management of irrigation with RW and deficit irrigation strategies, it is essential to identify the most appropriate and robust thermal indicator as well as the best time of day to perform the thermal readings [28].

In spite of the thermal measurements carried out at midday being generally used as a standard for the assessment of plant water status [3,24,26,35,48,49], in grapefruit, the data obtained at 10.00 GMT, best described the spatial variability throughout the experimental period, except for RW-RDI trees in Period 3, in which the Tc-Ta maximum values measured by IRTs in leaves in the upper part of the canopy were collected at 12.00 GMT (Figure 8B). This was likely due to the RW-RDI treatment maintaining the stomata partially open until that time. In our understanding, only one other study has reported that the temperature obtained earlier in the morning was less affected by background effects than that measured at noon, even though the study used airborne thermal imagery in olive trees [50].

The close behavior encountered between Tc-Ta and Tc with Ψ_{stem} ($p < 0.005$) (Table 4) confirmed the previous findings on the use of canopy temperature as the crop water status indicator in most orchards [18,48,51–53] including citrus [24] where the authors found higher correlations in Navelina orange trees ($r^2 = 0.75$). On the contrary, other authors such as those from Reference [13] reported on the difficulty of using Tc measurements obtained with fixed IRTs and normalized with air temperature (Tc-Ta) as a water stress indicator in citrus because they were poorly related with Ψ. A weak relationship between Tc-Ta and Ψ has also been reported in Navel Lane Late trees under RDI [22], and in Powell Navel oranges and Clemenvilla mandarins [25] in which Tc was obtained with a thermal camera.

In our work, the suitability of CWSI for assessing the water status in grapefruit was also observed in its correlation with Ψ_{stem} (Table 4), where the data from all experimental periods were pooled. CWSI showed good agreement with Ψ_{stem} ($R = 0.74$, $p < 0.005$). This R value was slightly higher than those obtained for the relationships between Tc, Tc-Ta, and Ψ_{stem} (Table 4).

In general, as our data demonstrated, the different seasonal indicators obtained by infrared thermometry had advantages and disadvantages, which must be taken into account when they are used in the field for saline and water stress monitoring. Regarding the simplicity and the time consuming aspects, the Tc and Tc-Ta would be more recommendable as a preliminary indicator of stress because they are easy to calculate [28]. However, climatic conditions more than CWSI influence these. Therefore, they can have major limitations for the remote sensing characterization of crop water status while the CWSI would be more robust especially under more variable environmental conditions throughout the day [28].

5. Conclusions

In grapefruit trees, the canopy temperature measured by infrared thermometry was higher than air temperature, which results in positive differences between Tc-Ta for a wide range of VPD during the middle hours of the day. The maximum values of Tc-Ta were found before midday.

The most significant correlations between Tc-Ta and VPD for establishing the Non Water Stressed Baseline (NWSB) were found in the early morning hours, when VPD was low and Tc-Ta values were high. The slopes of such correlations were positive. The thermal indicator that had the highest level of agreement with the stem water potential of the different treatments was CWSI even though Tc and Tc-Ta were significantly correlated.

In summary, in this work, the suitability of thermal indicators, mainly CWSI, throughout different seasonal periods was demonstrated in order to determine the water status of grapefruits under saline stress from reclaimed water and a water deficit period. Some of the aspects described in this paper are reported in the literature for the first time, which may include, on the one hand, the use of NWSBs with positive slopes for the CWSI calculation, and, on the other hand, the hourly and seasonal variation of NWSBs in citrus. Future research on the usefulness of thermometry to determine hourly changes within the same day is necessary.

Author Contributions: Data curation, C.R.T. and J.M.B.G. Formal analysis, C.R.T. Investigation, C.R.T., P.A.N.T., J.J.A.C., and E.N.N. Methodology, C.R.T., J.M.B.G., P.A.N.T., and E.N.N. Project administration, E.N.N. Resources, J.J.A.C. and E.N.N. Supervision, P.A.N.T. and E.N.N. Writing—original draft, C.R.T. Writing—review & editing, E.N.N.

Funding: This research was funded by a Spanish Ministry project CICYT (AGL2016-77282-C3-1-R) and Fundación Séneca (19903/GERM/15) granted to the authors.

Acknowledgments: The authors are grateful to the Spanish Ministry: CICYT (AGL2010-17553; AGL2013-49047-C2-2-R); Romero-Trigueros, C. acknowledge the financial support for Postdoctoral training and development fellowship (20363/PD/17) of Consejería de Empleo, Universidades y Empresa (CARM) by the Fundación Séneca—Agencia de Ciencia y Tecnología de la Región de Murcia.

Conflicts of Interest: The authors declare no conflict of interest.

References

1. Field, C.B.; Barros, V.R.; Dokken, D.J.; Mach, K.J.; Mastrandrea, M.D.; Bilir, T.E.; Bilir, M.; Chatterjee, K.L.; Ebi, Y.O.; Estrada, R.C.; et al. *IPCC, 2014: Climate Change 2014: Impacts, Adaptation and Vulnerability. Part A: Global and Sectoral Aspects. Contribution of Working Group II to the fifth Assessment Report of the Intergovernmental Panel on Climate Change*; Cambridge University Press: Cambridge, UK; New York, NY, USA, 2014.
2. ONU. *World Population Prospects. The 2017 Revision Key Findings and Advance Tables. Department of Economic and Social Affairs, Population Division*; Working Paper No. ESA/P/WP/248; United Nations Organization (ONU): New York, NY, USA, 2017.
3. Gonzalez-Dugo, V.; Zarco-Tejada, P.J.; Nicolás, E.; Nortes, P.A.; Alarcón, J.J.; Intrigliolo, D.S.; Fereres, E. Using high resolution UAV thermal imagery to assess the variability in the water status of five fruit tree species within a commercial orchard. *Precis. Agric.* **2013**, *14*, 660–678. [CrossRef]
4. Bastida, F.; Torres, I.; Abadía, J.; Romero-Trigueros, C.; Ruiz-Navarro, A.; Alarcón, J.J.; García, C.; Nicolás, E. Comparing the impacts of drip irrigation by freshwater and reclaimed wastewater on the soil microbial community of two citrus species. *Agric. Water Manag.* **2018**, *203*, 53–62. [CrossRef]
5. Nicolás, E.; Alarcón, J.J.; Mounzer, O.; Pedrero, F.; Nortes, P.A.; Alcobendas, R.; Romero-Trigueros, C.; Bayona, J.M.; Maestre-Valero, J.F. Long-term physiological and agronomic responses of mandarin trees to irrigation with saline reclaimed water. *Agric. Water Manag.* **2016**, *166*, 1–8. [CrossRef]
6. Romero-Trigueros, C.; Nortes, P.A.; Alarcón, J.J.; Nicolás, E. Determination of 15N stable isotope natural abundances for assessing the use of saline reclaimed water in grapefruit. *Environ. Eng. Manag. J.* **2014**, *13*, 2525–2530. [CrossRef]
7. Global Water Market. *Meeting the World's Water and Wastewater Needs Until 2020*; Global Water Intelligence: Oxford, UK, 2017; Volume 1, Issue 5.
8. ESAMUR. Entidad de Saneamiento y depuración de aguas residuales de la región de Murcia (Murcia Regional Government's Sanitation and Water Treatment Authority). 2017. Available online: http://www.esamur.com (accessed on 15 March 2017).
9. Pereira, B.F.F.; Heb, Z.L.; Stoffella, P.; Melfic, A.J. Reclaimed wastewater: Effects on citrus nutrition. *Agric. Water Manag.* **2011**, *98*, 1828–1833. [CrossRef]
10. Romero-Trigueros, C.; Nortes, P.A.; Pedrero, F.; Mounzer, O.; Alarcón, J.J.; Bayona, J.M.; Nicolás, E. Assessment of the sustainability of using saline reclaimed water in grapefruit in medium to long term. *Span. J. Agric. Res.* **2014**, *12*, 1137–1148. [CrossRef]
11. Romero-Trigueros, C.; Nortes, P.A.; Alarcón, J.J.; Hunink, J.E.; Parra, M.; Contreras, S.; Nicolás, E. Effects of saline reclaimed waters and deficit irrigation on Citrus physiology assessed by UAV remote sensing. *Agric. Water Manag.* **2017**, *183*, 60–69. [CrossRef]

12. Jones, H.G. Irrigation scheduling: Advantages and pitfalls of plant-based methods. *J. Exp. Bot.* **2004**, *55*, 2427–2436. [CrossRef]
13. Ballester, C.; Castel, J.; Jímenez-Bello, M.A.; Castel, J.R.; Intrigliolo, D.S. Thermographic measurement of canopy temperature is a useful tool for predicting water deficit effects on fruit weight in citrus trees. *Agric. Water Manag.* **2013**, *122*, 1–6. [CrossRef]
14. Ballester, C.; Zarco-Tejada, P.J.; Nicolás, E.; Alarcón, J.J.; Fereres, E.; Intrigiolo, D.S.; Gonzalez-Dugo, V. Evaluating the performance of xanthophyll, chlorophyll and structure-sensitive spectral indices to detect water stress in five fruit tree species. *Precis. Agric.* **2018**, *19*, 178–193. [CrossRef]
15. Jackson, R.D.; Idso, S.B.; Reginato, R.J.; Pinter, P.J. Canopy temperature as a crop water stress indicator. *Water Resour. Res.* **1981**, *17*, 1133–1138. [CrossRef]
16. Testi, L.; Goldhamer, D.A.; Iniesta, F.; Salinas, M. Crop water stress index is a sensitive water stress indicator in pistachio trees. *Irrig. Sci.* **2008**, *26*, 395–405. [CrossRef]
17. Wang, D.; Gartung, J. Infrared canopy temperature of early-ripening peach trees under postharvest deficit irrigation. *Agric. Water Manag.* **2010**, *97*, 1787–1794. [CrossRef]
18. Berni, J.A.J.; Zarco-Tejada, P.J.; Sepulcre-Canto, G.; Fereres, E.; Villalobos, F. Mapping canopy conductance and CWSI in olive orchards using high resolution thermal remote sensing imagery. *Remote Sens. Environ.* **2009**, *113*, 2380–2388. [CrossRef]
19. Barbagallo, S.; Consoli, S.; Russo, A. A one-layer satellite surface energy balance for estimating evapotranspiration rates and crop water stress indexes. *Sensors* **2008**, *9*, 1–21. [CrossRef]
20. Idso, S.B.; Jackson, R.D.; Reginato, R.J. Extending the "degree day" concept of plant phenological development to include water stress effects. *Ecology* **1978**, *59*, 431–433. [CrossRef]
21. Idso, S.B.; Jackson, R.D.; Pinter, P.J.; Reginato, R.J.; Hatfield, J.L. Normalizing the stress-degree-day parameter for environmental variability. *Agric. Meteorol.* **1981**, *24*, 45–55. [CrossRef]
22. Ballester, C.; Castel, J.; Testi, L.; Intrigliolo, D.S.; Castel, J.R. Can heat-pulse sap flow measurements be used as continuous water stress indicators of citrus trees? *Irrig. Sci.* **2013**. [CrossRef]
23. Ballester, C.; Jímenez-Bello, M.A.; Castel, J.R.; Intrigliolo, D.S. Usefulness of thermography for plant water stress detection in citrus and persimmon trees. *Agric. For. Meteorol.* **2013**, *168*, 120–129. [CrossRef]
24. García-Tejero, I.; Durán-Zuazo, V.H.; Muriel-Fernández, J.L.; Jiménez-Bocanegra, J.A. Linking canopy temperature and trunk diameter fluctuations with other physiological water status tools for irrigation scheduling in citrus orchards. *Funct. Plant Biol.* **2011**, *38*, 1–12. [CrossRef]
25. Zarco-Tejada, P.J.; Gonzalez-Dugo, V.; Berni, J.A.J. Fluorescence, temperature and narrowband indices acquired from a UAV platform for water stress detection using a micro-hyperspectral imager and a thermal camera. *Remote Sens. Environ.* **2012**, *117*, 322–337. [CrossRef]
26. Gonzalez-Dugo, V.; Zarco-Tejada, P.J.; Fereres, E. Applicability and limitations of using the crop water stress index as an indicator of water deficits in citrus orchards. *Agric. For. Meteorol.* **2014**, *198*, 94–104. [CrossRef]
27. Egea, G.; Padilla-Díaz, C.M.; Martínez, J.; Fernández, J.E.; Pérez-Ruiz, M. Assessing a crop water stress index derived from aerial thermal imaging and infrared thermometry in super-high density olive orchards. *Agric. Water Manag.* **2017**, *187*, 210–221. [CrossRef]
28. García-Tejero, I.; Rubio, A.E.; Viñuela, I.; Hernández, A.; Gutiérrez-Gordillo, S.; Rodríguez-Pleguezuelo, C.R.; Durán-Zuazo, V.H. Thermal imaging at plant level to assess the crop-water status in almond trees (cv. Guara) under deficit irrigation strategies. *Agric. Water Manag.* **2018**, *208*, 176–186. [CrossRef]
29. Gómez-Bellot, M.J.; Nortes, P.A.; Sánchez-Blanco, M.J.; Ortuño, M.F. Sensitivity of thermal imaging and infrared thermometry to detect water status changes in Euonymus japonica plants irrigated with saline reclaimed water. *Biosyst. Eng.* **2015**, *133*, 21–32. [CrossRef]
30. Sepaskhah, A.R.; Kashefipour, S.M. Evapotranspiration and crop coefficient of sweet lime under drip irrigation. *Agric. Water Manag.* **1995**, *27*, 331–340. [CrossRef]
31. Peel, M.C.; Finlayson, B.L.; McMahon, T.A. Updated world map of the Köppen-Geiger climate classification. *Hydrol. Earth Syst. Sci.* **2007**, *11*, 1633–1644. [CrossRef]
32. Pedrero, F.; Maestre-Valero, J.F.; Mounzer, O.; Nortes, P.A.; Alcobendas, R.; Romero-Trigueros, C.; Nicolás, E. Response of young 'Star Ruby' grapefruit trees to regulated deficit irrigation with saline reclaimed water. *Agric. Water Manag.* **2015**, *158*, 51–60. [CrossRef]
33. Fereres, E.; Goldhamer, D.A. Deciduous fruit and nut trees. In: Irrigation of agricultural crops. *Am. Soc. Agron.* **1990**, *30*, 987–1017.

34. Scholander, P.F.; Hammel, H.T.; Bradstreet, E.D.; Hemmingsen, E.A. Sap Pressure in Vascular Plants: Negative hydrostatic pressure can be measured in plants. *Science* **1965**, *148*, 339–346. [CrossRef]
35. Shackel, K.A.; Ahmadi, H.; Biasi, W.; Buchner, R.; Goldhamer, D.; Gurusinghe, S. Plant water status as an index of irrigation need in deciduous fruit trees. *HortTechnology* **1997**, *7*, 23–29. [CrossRef]
36. Cohen, Y.; Alchanatis, V.; Meron, M.; Saranga, Y.; Tsipris, J. Estimation of leaf potential by thermal imagery and spatial analysis. *J. Exp. Bot.* **2005**, *56*, 1843–1852. [CrossRef] [PubMed]
37. DeJongea, K.C.; Taghvaeian, S.; Trout, T.J.; Comas, L.H. Comparison of canopy temperature-based water stress indices for Maize. *Agric. Water Manag.* **2015**, *156*, 51–62. [CrossRef]
38. Ballester, C.; Castel, J.; Intrigliolo, D.S.; Castel, J.R. Response of clementina de nules citrus trees to summer deficit irrigation. Yield components and fruit composition. *Agric. Water Manag.* **2011**, *98*, 1027–1032. [CrossRef]
39. Veste, M.; Ben-Gal, A.; Shani, U. Impact of thermal stress and high VPD on gas exchange and chlorophyll fluorescence of citrus grandis under desert conditions. *Acta Hortic.* **2000**, *531*, 143–149. [CrossRef]
40. Villalobos, F.J.; Testi, L.; Moreno-Perez, M.F. Evaporation and canopy conductance of citrus orchards. *Agric. Water Manag.* **2009**, *96*, 565–573. [CrossRef]
41. Villalobos, F.J.; Testi, L.; Orgaz, F.; Garcia-Tejera, O.; Lopez-Bernal, A.; Gonzalez-Dugo, V.; Ballester-Lurbe, C.; Castel, J.R.; Alarcón-Cabañero, J.J.; Nicolás-Nicolás, E.; et al. Modelling canopy conductance and transpiration of fruit trees in Mediterranean areas: A simplified approach. *Agric. For. Meteorol.* **2013**, *171–172*, 93–103. [CrossRef]
42. Cohen, S.; Cohen, Y. Field studies of leaf conductance response to environmental variables in Citrus (orange). *J. Appl. Ecol.* **1983**, *20*, 561–570. [CrossRef]
43. Sepaskhah, A.R.; Kashefipour, S.M. Relationships between leaf water potential, CWSI, yield and fruit-quality of sweet lime under drip irrigation. *Agric. Water Manag.* **1994**, *25*, 13–22. [CrossRef]
44. Bellvert, J.; Zarco-Tejada, P.J.; Girona, J.; Fereres, E. Mapping crop water stress index in a "Pinot-noir" vineyard: Comparing ground measurements with thermal remote sensing imagery from an unmanned aerial vehicle. *Precis. Agric.* **2014**, *15*, 361–376. [CrossRef]
45. Hipps, L.E.; Asrar, G.; Kanemasu, E.T. A Theoretically-Based Normalization of Environmental-Effects on Foliage Temperature. *Agric. For. Meteorol.* **1985**, *35*, 113–122. [CrossRef]
46. Levy, Y.; Kaufmann, M.R. Cycling of leaf conductance in citrus exposed to natural and controlled environments. *Can. J. Bot.* **1976**, *54*, 2215–2218. [CrossRef]
47. Dzikiti, S.; Steppe, K.; Lemeur, R.; Milford, J.R. Whole-tree level water balance and its implications on stomatal oscillations in orange trees [Citrus sinensis (L.) Osbeck] under natural climatic conditions. *J. Exp. Bot.* **2007**, *58*, 1893–1901. [CrossRef]
48. García-Tejero, I.F.; Costa, J.M.; Egipto, R.; Lima, R.S.N.; Durán, V.H.; Lópes, C.; Chaves, M.M. Thermal data to monitor crop-water status in irrigated Mediterranean viticulture. *Agric. Water Manag.* **2016**, *176*, 80–90. [CrossRef]
49. Pou, A.; Diago, M.P.; Medrano, H.; Baluja, J.; Tardaguila, J. Validation of thermal indices for water status identification in grapevine. *Agric. Water Manag.* **2014**, *134*, 60–72. [CrossRef]
50. Sepulcre-Cantó, G.; Zarco-Tejada, P.J.; Jiménez-Munóz, J.C.; Sobrino, J.A.; De Miguel, E.; Villalobos, F.J. Detection of water stress in an olive orchard with thermal remote sensing imagery. *Agric. For. Meteorol.* **2006**, *136*, 31–44. [CrossRef]
51. Moran, M.S.; Clarke, T.R.; Inoue, Y.; Vidal, A. Estimating crop water deficit using the relation between surface-air temperature and spectral vegetation index. *Remote Sens. Environ.* **1994**, *49*, 246–263. [CrossRef]
52. García-Tejero, I.; Durán-Zuazo, V.H.; Arriaga, J.; Hernández, A.; Vélez, L.M.; Muriel-Fernández, J.L. Approach to assess infrared thermal imaging of almond trees under water-stress conditions. *Fruits* **2012**, *67*, 463–474. [CrossRef]
53. García-Tejero, I.; Hernández, A.; Padilla-Díaz, C.M.; Diaz-Espejo, A.; Fernández, J.E. Assessing plant water status in a hedgerow olive orchard from thermography at plant level. *Agric. Water Manag.* **2017**, *188*, 50–60. [CrossRef]